

Response time central-limit and failure rate estimation for stationary periodic rate monotonic real-time systems

Kevin Zagalo¹ and Avner Bar-Hen²

¹Inria, INSA Lyon, CITI, UR3720, Villeurbanne, France

²Cnam, Paris, France

Abstract

Real-time systems consist of a set of tasks, a scheduling policy, and a system architecture, all constrained by timing requirements. Many everyday embedded systems, within devices such as airplanes, cars, trains, and spatial probes, operate as real-time systems. To ensure safe failure rates, response times—the time required for the execution of a task—must be bounded. Rate Monotonic real-time systems prioritize tasks according to their arrival rate. This paper focuses on the use of the central limit of response times built in [44] and an approximation of their distribution with an inverse Gaussian mixture distribution. The distribution parameters and their associated failure rates are estimated through a suitable re-parameterization of the inverse Gaussian distribution and an adapted Expectation-Maximization algorithm. Extensive simulations demonstrate that the method is well-suited for the approximation of failure rates. We discuss the extension of such method to a chi-squared independence test adapted to real-time systems.

Keywords: EM algorithm ; Inverse Gaussian mixture ; Rate-monotonic; Real-time systems

1 Introduction

The increasing demand for new functionalities in embedded systems within automotive, avionics and space industries is driving an increase in the performance required in embedded processing units [21]. Real-time systems are computing systems in which tasks must meet their time requirements that we refer as deadlines. If a task do not meet its deadline, it is considered a failure. Embedded systems usually use little energy and computing resources, thus have a specific design with a micro-controller architecture and a set of task running on it [19].

An important part of this design is to associate a processing unit to a given task set. The time taken by the system to respond to an input and provide the output or display the updated information is known as the end-to-end latency. It is composed of two main parts: the communication of the data from the sensors to a task; and the time needed to complete the workload of the task itself called *response time*. In this paper we study response times, and more specifically, we estimate the probability that the response time of a task is larger than a predefined threshold. During run-time, each instance of the tasks compete for processing time on the basis of their priority. To ensure that every task is executed within their specified timing constraints, computation resources are allocated to different tasks according to their priority. Depending on the device, missing a deadline can be very costly or even catastrophic. Therefore a classical problem is the study of the performance of the worst-case scenario, *i.e.*, the scenario producing the largest response times. This method is generally efficient but it forces designers to overestimate the quantity of processing unit necessary to run a task set. Since the complexity of real-time systems is increasing, the worst-case scenario often becomes unrealistic and over-estimation of Worst-Case Response Time (WCRT) increases drastically. A way to soften resource requirements is to allow a (low) failure rate for each task, such that the probability that a deadline is missed is bounded by this failure rate.

Related work Historically, the distribution of response time have been computed in a closed form for periodic real-time systems in discrete time with discrete execution times in [9]. This approach is based on the convolution operator, and provides an iterative method to compute the exact distribution of response times. However, this convolution operator has a high complexity [26]. This complexity might not be a problem in the design part of a real-time system, however we aim to approach the timing analysis as part of the scheduling process itself. This complexity is the main reason why the concentration inequalities have been widely used to bound failure rates [5, 13–15, 25, 27, 41].

Failure rates are used in the design process of real-time systems in order to provide quality of service metrics. We propose in this work a first step into the incorporation of the failure rates estimate in the scheduling process itself. It opens the possibility of an adaptive scheduling method taking failure rates into account, by estimating during run-time the distribution and/or the component of the mixture where response times belong. This kind of adaptive algorithms are studied in [32, 37, 43] and the impact of such prediction within the scheduling algorithm is studied in [16]. We do not build such adaptive algorithm in this work.

The starting point of the failure rate estimation provided in this work is the central limit of response times built in [44], pushing the inverse Gaussian (IG) distribution as a natural candidate to approximate response time distributions. The IG family is a natural choice for the statistical modelling of positive and right-skewed distributions, see [11, 40]. It is used in many fields, such as industrial degradation modelling, psychology, and many others like hydrology,

market research, biology, ecology, etc. *c.f.*, [36].

Contributions Three methods to approach the failure rates are compared in this paper : empirical failure rates, a theoretical bound on failure rates and an estimation of the failure rates. Note that only the theoretical bounds can determine safely the feasibility of a real-time system, *i.e.*, failure rates equal to 0. We emphasize the fact that the estimated failure rates should not in any case be considered as a measure of reliability of the system. In Section 2, stationary rate monotonic real-time systems are introduced. A theoretical bound on failure rates-the Hoeffding bound-is provided as a baseline. We then propose a suited parameterization of the IG distribution in Section 3 adapted to response times, in the form of (9). This reparametrization is based on the central limit-like result given in [44]. Using an adapted EM algorithm, we estimate the parameters of a mixture of IG probability density functions (p.d.f.). Failure rates are estimated through this parameterization. Finally in Section 4 we apply the foregoing method to simulated and real data. All proofs are provided in appendices.

2 Stationary periodic rate monotonic real-time systems

In this paper we consider *periodic* tasks, meaning that an instance of each task is periodically released at a given rate, and a single core system, *i.e.*, only one task is processed at a time. Hence a real-time system is referred to only with its task set. The deadlines are *implicit*, *i.e.*, an instance of a task should finish its execution before the next instance of the same task in order to respect its timing requirements. Note that all notations are summarized in Table 1.

2.1 Model

Let us consider a periodic real-time system $\Gamma = (\gamma_i)_i$. Without loss of generality, the task indices are ordered by decreasing priority: If $k < i$, γ_k preempts γ_i if both γ_i and γ_k are activated. Task prioritization ensures that the most critical and time-sensitive tasks are completed first to meet deadlines. A task γ_i is characterized by:

1. its *execution time* C_i , with non-negative and finite support $[c_i^{min}, c_i^{max}]$.
2. its *period* $p_i > 0$. We note $\lambda_i = 1/p_i$ the rate of arrival of γ_i . p_i is also its *deadline*, *i.e.*, the maximum time given to the task γ_i to be processed.

We suppose that the execution times of the jobs and tasks are statistically independent. All results strongly depend on this assumption.

Let us first introduce some concepts that will be used throughout this paper.

Utilization Let us define *k-level mean utilization* of Γ as

$$u_k = \sum_{i=1}^k \lambda_i \mathbf{E}[C_i].$$

Tab. 1: Notations used throughout the paper.

Γ	task set
γ_i	task of index i
$\gamma_{i,j}$	j -th job of the task of index i
Δ_i	failure rate of the task of index i
$\Delta_i^{(n)}$	empirical failure rate of the task of index i
Δ_i^{IG}	approximated failure rate of the task of index i
C_i	execution time of the task of index i
$C_{i,j}$	execution time of the j -th job of the task of index i
f_i	p.d.f. of the execution time of the task of index i
u_i	mean utilization of level i of Γ
u_i^{max}	maximum utilization of level i of Γ
v_i	standard deviation of level i of Γ
v_i^{max}	maximum deviation of level i of Γ
$R_{i,j}$	response time of the j -th job of the task of index i
R_i	response time of the mixture of all jobs of the task of index i
h_i	p.d.f. of the response time of the mixture of all jobs of the task of index i
$A_{i,j}$	arrival time of the j -th job of the task of index i
N_i	counting process of the task of index i
O_i	offset -arrival time of the first job- of the task of index i
p_i	time separating two consecutive jobs of the task of index i
λ_i	rate of arrival of the jobs of the task of index i
$\beta_{i,j}$	accumulated backlog of jobs of index strictly lower than i at time $A_{i,j}$
$\hat{\beta}_{i,j}$	approximation of $\beta_{i,j}$
$m_{i,j}$	distribution of the cumulated backlog of jobs of index strictly lower than i at time $A_{i,j}$
π_i	distribution of the cumulated backlog of jobs of index strictly lower than i
$\pi_{i,k}$	weight of the k -th component of the mixture of the response time of the task of index i
$\hat{\pi}_{i,k}$	approximation of $\pi_{i,k}$
K_i	degree of freedom of the approximated failure rate for the task of index i
$\psi(r; \xi, \delta)$	p.d.f. of the IG distribution of mean ξ and shape δ
$\mu_i(\beta)$	mode of the IGce distribution of mean $\frac{\beta}{1-u_i}$ and shape $\frac{\beta^2}{v_i^2}$
ν_i	variation coefficient of the IG distribution of mean $\frac{\beta}{1-u_i}$ and shape $\frac{\beta^2}{v_i^2}$
$\tilde{\psi}(r; \mu, \nu)$	p.d.f. of the reparametrized IG distribution of mode μ and variation coefficient ν
$\psi_i(r; \beta)$	p.d.f. of the IG distribution of mean $\frac{\beta}{1-u_i}$ and shape $\frac{\beta^2}{v_i^2}$
$\Psi(r; \xi, \delta)$	c.d.f. of the IG distribution of mean ξ and shape δ
Φ	c.d.f. of the $\chi^2(1)$ distribution

The k -level mean utilization takes into account all tasks with higher or equal priority than the task γ_k . Let also define the k -level maximum utilization of Γ as

$$u_k^{max} = \sum_{i=1}^k \lambda_i c_i^{max}.$$

Deviation Let us define the k -level deviation of Γ as

$$v_k = \left(\sum_{i=1}^k \lambda_i \mathbf{E}[C_i^2] \right)^{1/2}.$$

The k -level deviation takes into account all tasks with higher or equal priority than the task γ_i . Let also define the k -level maximum deviation of Γ as

$$v_k^{max} = \left(\sum_{i=1}^k \lambda_i (c_i^{max} - c_i^{min})^2 \right)^{1/2}.$$

Jobs A job $\gamma_{i,j}$ is the j -th instance of the task γ_i . $C_{i,j}$ is its execution time of p.d.f. f_i and $A_{i,j}$ is its arrival time such that

$$\forall j \geq 1, A_{i,j+1} - A_{i,j} = p_i. \quad (1)$$

This translates into the time between two consecutive of jobs being p_i with probability 1.

Stationarity We assume the *stationarity* of Γ , that we define as the stationarity of all demand processes

$$W_i(t) = \sum_{j=1}^{N_i(t)} C_{i,j}$$

where $N_i(t) = \sum_{j=1}^{\infty} \mathbf{1}_{[0,t]}(A_{i,j})$ is the process counting the jobs of the task γ_i arrived before instant $t \geq 0$. This means that we assume that the distribution of the number of jobs arrived in an interval $[s, t]$ is the same as the one over any time interval $[u, u + t - s]$ of size $t - s$, *i.e.*, $\mathbf{P}(N_i(t) - N_i(s) = n) = \mathbf{P}(N_i(t - s) = n)$. Since the arrival process $A_i = (A_{i,j})_j$ verifies (1), it is easy to verify that it suffices that the first arrival (*a.k.a.* offset) $O_i = A_{i,1}$ is continuously and uniformly distributed between 0 and p_i . Note that $N_i(t) = \lceil \lambda_i(t - O_i)^+ \rceil^1$ and $\mathbf{E}[N_i(t)] = \lambda_i t$, and that $\sum_i N_i$ is not stationary in general. From the stationarity of $N_i(t)$ and the fact that the $(C_{i,j})_j$ are i.i.d. implies that $W_i(t + s) - W_i(s)$ has the distribution of $W_i(t)$, *i.e.* W_i is stationary. The sum $\sum_i W_i$ is not stationary in general either.

¹ where $x^+ = \max(0, x)$.

Backlog In order to make the analysis simpler, we will make the assumption that whenever a job misses its deadline, it is considered useless and is discarded from the system. This will ensure that the worst-case scenario is the simultaneous activation of all tasks, in the sense that it provides the largest response time. The backlog of the task γ_i is defined as the amount of time required at a given time to terminate all active jobs of the task γ_i . The backlog process of a task γ_i can be defined as

$$\beta_i(t) = C_{i,N_i(t)} - \int_{A_{i,N_i(t)}}^t \mathbf{1}(\beta_i(s) > 0) \prod_{k=1}^{i-1} \mathbf{1}(\beta_k(s) = 0) ds.$$

The backlog process was first introduced in real-time system timing analyses in [9] in the discrete case with no discarding, and [44] in the continuous case, where it is shown that this backlog process is ergodic, if and only if $u_i < 1$, *i.e.*, it converges with probability 1. The discrete time analysis provided in [9] induced a literature based on the convolution operator. In the discrete time case, the distribution of $\beta_i(A_{i,j+1})$ has been extensively studied using the convolution of the p.d.f. of each individual execution time at each arrival time, as well as the distribution of the limit $\lim_{t \rightarrow \infty} \beta_i(t)$. Nevertheless, the workload that needs to be terminated before a job $\gamma_{i,j}$ is $\sum_{k=1}^{i-1} \beta_k(A_{i,j})$. Unfortunately, the cumulated backlog process $\sum_{k=1}^{i-1} \beta_k$ is not stationary in general.

Response times The *response time* of $\gamma_{i,j}$ is denoted $R_{i,j}$, and is the time elapsed between $A_{i,j}$ and the end of its execution. Thus a response time of a job is the sum of the execution time of this job and the execution times of higher priority jobs that preempt it, see Figure 1. Hence, it depends on the scheduling policy. For a fixed-priority discarding scheduling policy, the response time $R_{i,j}$ can be written as

$$R_{i,j} = \inf\{t > 0 : \beta_i(A_{i,j} + t) = 0\}. \quad (2)$$

The relative deadline of a task, *i.e.*, its maximum allowed response time, is equal to its period. This means that the response time $R_{i,j}$ of the job $\gamma_{i,j}$ should be lower than p_i . Therefore, the absolute deadline of $\gamma_{i,j}$ is $A_{i,j+1}$. Note that the response times are dependent on the scheduling policy used with the system. In this paper we use the RM scheduling policy that we define in the following section. A job is discarded if it misses its deadline, and as we consider implicit deadlines, there can be at most one job per task activated simultaneously.

The parametric estimation provided in this work relies on the convergence in distribution built in [44].

Proposition 1 (Central limit). *Given a backlog $\sum_{k=1}^i \beta_k(A_{i,j}) = \beta$, the response time $R_{i,j}$ converges in distribution to an inverse Gaussian distribution when the mean utilization u_i goes to 1 from below, *i.e.**

$$\mathbf{P}(R_{i,j} > t \mid \sum_{k=1}^i \beta_k(A_{i,j}) = \beta) \underset{u_i \rightarrow 1^-}{\simeq} 1 - \Psi\left(t; \frac{\beta}{1 - u_i}, \frac{\beta^2}{v_i^2}\right) \quad (3)$$

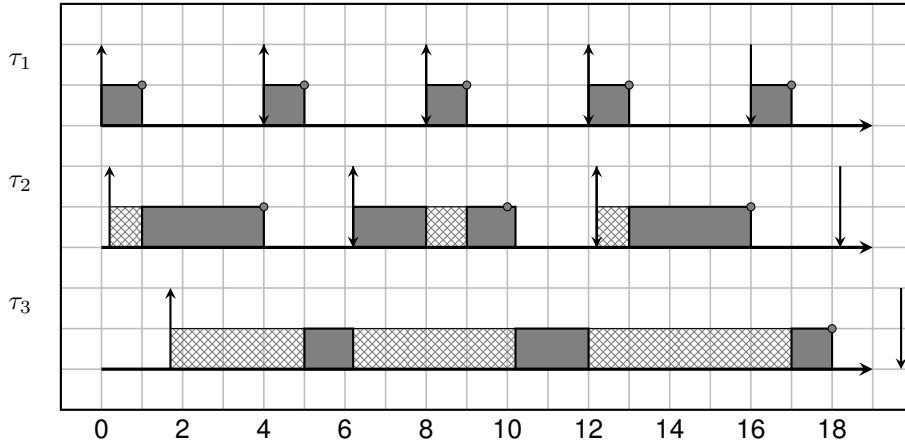


Fig. 1: Example of a static-priority schedule with $O_1 = 0, C_1 = 1, p_1 = 4, O_2 = 0.2, C_2 = 3, p_2 = 6, O_3 = 1.7, C_3 = 4, p_3 = 18$. The higher priority tasks stop the execution of tasks if needed. Thus, the response time is time between the release and the end of a job, taking the jobs of higher priority tasks into account. Corner dots represent the end of a job, up-arrows their arrival time, down arrows their absolute deadlines.

where $\Psi(r; \xi, \delta)$ is the c.d.f. of the inverse Gaussian distribution of mean ξ and shape δ .

Proof. See Appendix A. □

Failure rate The *failure rate* of the task $\gamma_i \in \Gamma$ is defined by

$$\Delta_i = \lim_{n \rightarrow \infty} \frac{1}{n} \sum_{j=1}^n \mathbf{P}(R_{i,j} > p_i). \quad (4)$$

Thus finding an analytical expression of the p.d.f. of response times permits to determine the failure rates. Moreover, in [44], it is proven that in the case of stationary real-time systems, the sequence $(R_{i,j}, j \in \mathbb{N})$ is stationary. In terms of failure rate, this means that the sum in (4) is finite, *i.e.*, $\Delta_i = \frac{1}{K} \sum_{j=1}^K \mathbf{P}(R_{i,j} > p_i)$ for some integer $K > 0$. We estimate this number of components K , that we refer to as degree of freedom, in Section 3.4.

Rate Monotonic We consider a real-time system Γ ordered by decreasing priority order and scheduled with the RM policy: Γ is such that priorities are ordered decreasingly with the rates, *i.e.*, $\lambda_i \geq \lambda_{i+m}$ for any $m \geq 0$. RM is optimal for real-time systems using static-priorities and implicit deadlines [2]. By optimal, we mean that if RM fails to schedule Γ , then all static-priority

scheduling policies also fail to make Γ feasible. If $u_i > 1$, $\gamma_i \in \Gamma$ is not feasible, *i.e.*, $\Delta_i = 1$, *c.f.*, [44]. The seminal work of Liu and Layland [24] provides a sufficient condition for the feasibility of any system with finite supports of execution times using the *k-level maximal utilization*. Whenever

$$u_k^{max} < k(2^{1/k} - 1) \quad (5)$$

the task set Γ is such that for all $i \leq k$, and all $j \in \mathbb{N}$, the probability of a failure $\mathbf{P}(R_{i,j} > p_i)$ is equal to zero [24, Theorem 5], and thus $\Delta_1 = \dots = \Delta_k = 0$. Moreover, while $u_k^{max} < 1$ there exists a scheduling policy, with dynamic priorities that can satisfy the feasibility of the task γ_i [24]. Hence there are two phase transitions, one at $u_k^{max} > \log(2)^2$ where failures *can* happen, and one at $u_k^{max} > 1$ where failures *must* happen. As proven in [9], the necessary condition for the feasibility of a task γ_k is that the mean utilization u_k is less than one. Hence, there is a room for an improvement between the necessary condition provided in [9], *c.f.*, $u_k < 1$ and the sufficient condition $u_k^{max} < k(2^{1/k} - 1)$. In particular in the case where $u_k < 1$ and $u_k^{max} > 1$ as we see in Figure 2.

2.2 Hoeffding bound for stationary periodic rate monotonic real-time systems

Before using inference methods, we provide the Hoeffding bound associated to the setup as a baseline.

Proposition 2 (Hoeffding bound). *Let Γ be a stationary periodic rate-monotonic real-time system as defined in Section 2.1, $\gamma_i \in \Gamma$ and suppose $u_i < 1, u_i^{max} > i(2^{1/i} - 1)$. Then if $p_i > \frac{2 \sum_{k=1}^i \mathbf{E}[C_k]}{1 - u_{i-1}}$,*

$$\Delta_i \leq \exp \left(-9\lambda_i \left(\frac{\sum_{k=1}^i \mathbf{E}[C_k]}{v_i^{max}} \right)^2 \right).$$

Proof. See Appendix B. □

Note that the Hoeffding bound approach has been used in [41] in a different context. We use the Hoeffding bound to compare it to the results of the estimation built in the next sections. Indeed, the failure rate estimation provided in this work are not guaranteed, they are estimations that could be for example incorporated in a predictive scheduling algorithm [32]. We do not investigate such algorithm, but provide a well defined and parametrized method to make one.

3 Inverse Gaussian distribution and response times

The arrival of jobs can be represented as a queueing process with a deterministic activation rate (D), a general execution time distribution (G), and one server (1)

² The bound usually used in the converse inequality (5) is $\lim_{k \rightarrow \infty}^{\uparrow} k(2^{1/k} - 1) = \log(2)$.

since we consider a single process scheme with fixed priorities (FP). This model is widely used in the analysis of various types of service systems such as call centers, banks, or hospitals and has been widely studied [3]. An approximation of response times is determined by using the *heavy-traffic assumption* [10, 22, 44] on the D/G/1/FP queues associated to the point processes $(A_i)_i$ ordered by priority, and the execution time distributions which have a finite support, which permits to approximate the size of a queue with a Brownian motion.

In [44], authors propose to approximate response time distributions in the fixed-priority setup, with inverse gaussian distributions, by conditioning the backlog process values. They provide a result analogous to a central limit theorem on response times, using heavy-traffic theory [23] : if a job of priority i starts with a backlog β , the p.d.f. of its response time tends to

$$\psi(r; \xi, \delta) = \sqrt{\frac{\delta}{2\pi r^3}} \exp\left(-\frac{\delta(r - \xi)^2}{2r\xi^2}\right), r \geq 0$$

when u_i tends to 1 from below, and where $\psi(r; \xi, \delta)$ is the p.d.f. of the inverse Gaussian distribution of mean ξ and shape δ . In this paper, we provide an approximation of the failure rates associated to this central limit in the case of a rate monotonic scheduling policy. The key parameter β is directly related to the arrival of the previous tasks and can be estimated from the empirical data. In [44], authors prove that when the mean utilization u_i is smaller than 1, the distribution of response times can be approximated by a mixture of IG distributions (6), *i.e.*, they provide a central limit theorem for response times.

$$\frac{\mathbf{P}(R_{i,j} \in [r, r + dr])}{dr} \underset{u_i \rightarrow 1^-}{\simeq} \int_0^\infty \psi\left(r; \frac{\beta}{1 - u_i}, \frac{\beta^2}{v_i^2}\right) m_{i,j}(d\beta) \quad (6)$$

where $m_{i,j}$ is a probability measure on backlogs that we consider unknown. The purpose of finding the failure rate is to quantify the quality of the scheduling. Empirical measurements of response times however are not sufficient, as they are only a fraction of the possible values. Inference methods are used in the purpose of quantifying failure rates from measurements taking into account the shape that response times distributions should have. Nevertheless, the estimation method provides no strict bound, as the Hoeffding bound (Proposition 2) does for example, but rather gives a scale of what to expect in terms of failure rates when using inference methods coupled with measurement-based methods.

3.1 Response time IG mixture model

In this section, we derive the foregoing central limit using the approximation in (6). Consider a stationary periodic rate monotonic real-time system Γ , and for $\gamma_i \in \Gamma$ suppose $u_i < 1$, $u_i^{max} > i(2^{1/i} - 1)$. Let R_i be the variable of p.d.f.

$$h_i(r) = \lim_{n \rightarrow \infty} \frac{1}{n} \sum_{j=1}^n \frac{\mathbf{P}(R_{i,j} \in [r, r + dr])}{dr} \quad (7)$$

such that $\Delta_i = \int_{p_i}^{\infty} h(r)dr$. Using both (6) and (7) gives the IG approximation

$$h_i(r) \underset{u_i \rightarrow 1^-}{\simeq} \int_0^{\infty} \psi \left(r; \frac{\beta}{1-u_i}, \frac{\beta^2}{v_i^2} \right) \pi_i(d\beta) \quad (8)$$

where the stationary distribution of backlogs $\pi_i = \lim_{n \rightarrow \infty} \frac{1}{n} \sum_{j=1}^n m_{i,j}$ exists and is unique according to [44] in the continuous time case, and [9] in the discrete time case. From there, and using the ergodicity of backlogs, we can approximate the integral in (8) by the finite sum

$$h(r; \boldsymbol{\pi}_i, \boldsymbol{\beta}_i) = \sum_{k=1}^{K_i} \pi_{i,k} \psi \left(r; \frac{\beta_{i,k}}{1-u_i}, \frac{\beta_{i,k}^2}{v_i^2} \right) \quad (9)$$

by finding the appropriate parameters $(\boldsymbol{\pi}_i, \boldsymbol{\beta}_i, K_i)$, which we find by maximizing the likelihood of an IG mixture model. Hence, we get an approximation of the failure rate Δ_i , namely

$$\Delta_i^{\text{IG}} = \int_{p_i}^{\infty} h(r; \boldsymbol{\pi}_i, \boldsymbol{\beta}_i) dr. \quad (10)$$

By developing (10) we get the following approximated failure rate,

$$\Delta_i^{\text{IG}} = \sum_{k=1}^{K_i} \pi_{i,k} \left[1 - \Psi \left(p_i; \frac{\beta_{i,k}}{1-u_i}, \frac{\beta_{i,k}^2}{v_i^2} \right) \right] \quad (11)$$

where we estimate $(\boldsymbol{\pi}_i, \boldsymbol{\beta}_i, K_i)$ the following sections.

3.2 Re-parameterized IG distribution for response times

The purpose of this section is to provide the efficient distribution family for an approximation of response times and an adapted EM algorithm to estimate the parameters of this approximation. This adapted re-parameterization of the IG distribution reduces the number of parameters of the mixture model. This increases the speed of convergence the estimation algorithm as well as the stability of the estimates. Furthermore, as underlined in [31], the log-likelihood of the IG distribution has flat regions thus the EM algorithm has very tiny variations. Reducing the number of parameters addresses a part of this problem. A second reduction of this problem is the use of the Aitken acceleration procedure [1].

In [31], the author introduces a modified version of the IG distribution of parameters (ξ, δ) , using its *variability coefficient* $\nu = \xi^2/\delta$ and its mode $\mu = (\xi^2 + 2.25\nu^2)^{1/2} - 1.5\nu$ instead of the shape and the mean. This re-parameterized IG distribution (rIG), $\tilde{\psi}$, of parameters (μ, ν) is defined by the probability density function

$$\tilde{\psi}(r; \mu, \nu) = \sqrt{\frac{\mu(3\nu + \mu)}{2\pi\nu r^3}} \exp \left\{ -\frac{\left(r - \sqrt{\mu(3\nu + \mu)} \right)^2}{2\nu r} \right\}$$

With the rIG distribution applied to the form that take the parameters of the distributions of response times, one can see that only the mode is sensitive to the mixture provided in (9). The variability coefficient of an IG distribution of mean $\beta/(1 - u_i)$ and shape $(\beta/v_i)^2$ is

$$\nu_i = \frac{v_i^2}{(1 - u_i)^2}$$

and its mode is

$$\mu_i(\beta) = \sqrt{\left(\frac{\beta}{1 - u_i}\right)^2 + \frac{9\nu_i^2}{4}} - \frac{3\nu_i}{2}$$

so that

$$\psi_i(x; \beta) = \tilde{\psi}(x; \mu_i(\beta), \nu_i) = \psi\left(r; \frac{\beta}{1 - u_i}, \frac{\beta^2}{v_i^2}\right)$$

is the probability density function of an rIG distribution of mode $\mu_i(\beta)$ and variability ν_i . Therefore the variability of the component of the mixture of IG distributions does not depend on the backlog β .

3.3 Expectation-Maximization : estimating the backlog

In this section we present an adaptation of the maximum likelihood estimator (MLE) proposed by [31] for real-time systems (π_i, β_i) . Both are implemented in the Python language in the library `rInverseGaussian`³. We study first the case where a one-component mixture is sufficient to estimate response time distributions.

See [11] for the classical MLE of IG distributions. We know from [11, Eq. (10)] that the mean of an IG distribution is the empirical mean $\frac{1}{n} \sum_{j=1}^n R_{i,j}$. Furthermore, we are looking for estimating the mean $\frac{\beta}{1 - u_i}$. Since we already know u_i , we get the result by estimating $\frac{\beta}{1 - u_i}$ with $\frac{1}{n} \sum_{j=1}^n R_{i,j}$. When $K_i = 1$, $\pi_{i,1} = 1$ and we have the MLE

$$\hat{\beta}_i = \frac{1 - u_i}{n} \sum_{j=1}^n R_{i,j}.$$

thanks to the strong law of large numbers. When more than one components are to be estimated, we introduce an adapted EM algorithm to maximize the likelihood of the model, derived from the algorithm proposed in [31]. An EM algorithm is an algorithm which maximizes the likelihood of a random variable iteratively by finding the best suited parameters to describe this random variable's distribution. It is composed of two steps: the E-step which builds the likelihood of a fixed sample (of response times in our case); and the M-step which maximizes this likelihood by computing the best suited parameter (the backlog in our case). In our case, the distribution is a mixture, where EM the

³ <https://github.com/kevinzagalo/rInverseGaussian>

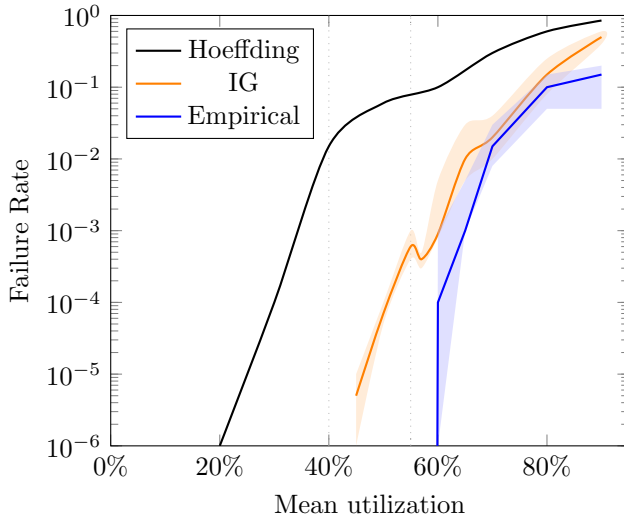


Fig. 2: Utilization against the failure rates of the IG estimation $(u_i, \Delta_i^{\text{IG}})_i$ in orange, the Hoeffding bound in black, and the empirical failure rates $(u_i, \Delta_i^{(n)})_i$ in blue, over a sample of $n = 10^6$ response times per task simulated on SimSo. The two dotted lines correspond to $u_i^{\text{max}} > \log(2)$ and $u_i^{\text{max}} > 1$. The colored surface surrounding the solid lines are the minimum and maximum failure rates produced by the simulations. Simulations are done twice for two task sets simulated from the same setup given in Table 2.

algorithm determines by itself which component of the mixture is best to describe the given sample in the E-step. It does so by computing a latent variable indicating in which component the sample is the most likely be in, as well as the weight of each of these components. EM algorithms for IG mixture models are widely studied [31]. However we provide the derivatives associated to the minimization problem that the EM algorithm solves in (14). The EM algorithm is adapted to the reparametrization introduced in the latter section.

Given a n -sample of response times, the complete-likelihood of the mixture model [28] associated to γ_i can be written as

$$L_c(\mathbf{Z}_i, \boldsymbol{\pi}_i, \boldsymbol{\beta}_i) = \prod_{j=1}^n \prod_{k=1}^{K_i} [\pi_{i,k} \psi_i(r_j; \beta_{i,k})]^{Z_{i,j,k}}$$

where $Z_{i,j,k} \in \{0, 1\}$ is the latent variable that indicates if $R_{i,j}$ is in the k -th mixture component, and the complete log-likelihood $\ell_c = \log L_c$ is

$$\ell_c(\mathbf{Z}_i, \boldsymbol{\pi}_i, \boldsymbol{\beta}_i) = \ell_{c_1}(\mathbf{Z}_i, \boldsymbol{\pi}_i) + \ell_{c_2}(\mathbf{Z}_i, \boldsymbol{\beta}_i)$$

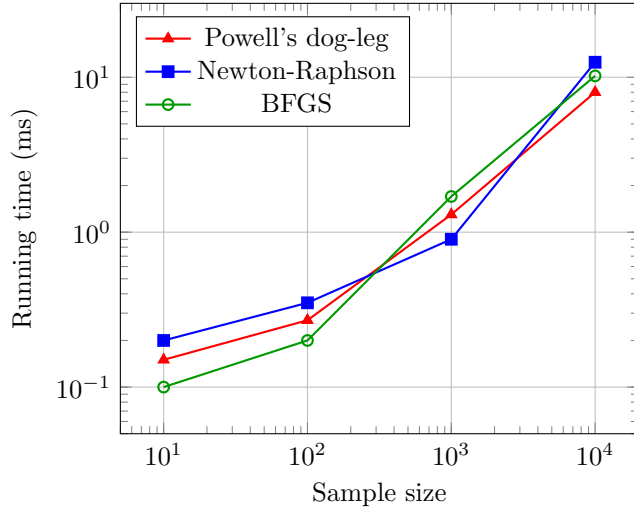


Fig. 3: Running time of the EM algorithm, using various Newton-like minimization algorithms to solve (13). All three methods appear to be equivalent.

where

$$\ell_{c_1}(\mathbf{Z}_i, \boldsymbol{\pi}_i) = \sum_{j=1}^n \sum_{k=1}^{K_i} Z_{i,j,k} \log \pi_{i,k}$$

and

$$\ell_{c_2}(\mathbf{Z}_i, \boldsymbol{\beta}_i) = \sum_{j=1}^n \sum_{k=1}^{K_i} Z_{i,j,k} \log \psi_i(r_j; \beta_{i,k})$$

which leads to the following EM algorithm. Note that j sums over the response times in the n -sample, k sums over the K_i components of the mixture and i is fixed and is the index of the task of interest. The degree of freedom K_i is estimated in the following section.

E-step For the $(s+1)$ th step of the EM algorithm, $\mathbf{z}_i^{(s)}$ the conditional expectation of \mathbf{Z}_i given $(\boldsymbol{\pi}_i, \boldsymbol{\beta}_i) = (\boldsymbol{\pi}_i^{(s)}, \boldsymbol{\beta}_i^{(s)})$ is given by

$$z_{i,j,k}^{(s)} = \frac{\pi_{i,k}^{(s)} \psi_i(r_j; \beta_{i,k}^{(s)})}{h(r_j; \boldsymbol{\pi}_i^{(s)}, \boldsymbol{\beta}_i^{(s)})}$$

M-step For the $(s+1)$ th step of the EM algorithm, $\ell_{c_1}(\mathbf{z}_i^{(s)}, \cdot)$ is maximized by

$$\pi_{i,k}^{(s+1)} = \frac{1}{n} \sum_{j=1}^n z_{i,j,k}^{(s)}, k = 1, \dots, K_i \quad (12)$$

and maximizing ℓ_{c_2} with respect to β is maximizing each of the K_i expressions

$$\sum_{j=1}^n z_{i,j,k}^{(s)} \log \psi_i(r_j; \beta_{i,k}), k = 1, \dots, K_i$$

using Newton-like algorithms (*c.f.*, Figure 3) to solve

$$\nabla \ell_c = 0 \quad (13)$$

Then with $\frac{\partial \log \psi_i}{\partial \beta}(r; \beta) = \frac{\partial \mu_i}{\partial \beta}(\beta) \frac{\partial \log \tilde{\psi}}{\partial \mu}(r; \mu_i(\beta), \nu_i)$ and the derivatives given in (14). Eq. (13) is equivalently solved by (12) and the solutions of

$$\sum_{j=1}^n z_{i,j,k}^{(s)} \frac{\partial \log \psi_i}{\partial \beta}(r_j; \beta_{i,k}) = 0, \forall k = 1, \dots, K_i$$

Criteria to stop the EM algorithm In order to stop the algorithm, the author in [31] proposes the *Aitken acceleration* to stop the algorithm and studies its efficiency. The Aitken acceleration at iteration $s + 1$ is given by

$$a^{(s+1)} = \frac{\ell^{(s+2)} - \ell^{(s+1)}}{\ell^{(s+1)} - \ell^{(s)}}$$

where $\ell^{(s)}$ is the observed-data log-likelihood from iteration s . The limit ℓ_∞ of the sequence of values of the log-likelihood is

$$\ell_\infty^{(s+2)} = \ell^{(s+1)} + \frac{\ell^{(s+2)} - \ell^{(s+1)}}{1 - a^{(s+1)}}.$$

The EM algorithm is considered to have converged if

$$|\ell_\infty^{(s+2)} - \ell_\infty^{(s+1)}| < \varepsilon$$

with a tolerance $\varepsilon > 0$.

Initialization We initialize the algorithm with a k -means clustering as suggested in [31], and do not investigate the impact of the initialization.

$$\begin{aligned} \frac{\partial \log \tilde{\psi}}{\partial \mu}(r; \mu, \nu) &= -\frac{3}{2r} - \frac{\mu}{r\nu} + \frac{1}{3\nu + \mu} + \frac{3\nu}{2\mu(3\nu + \mu)} + \frac{\sqrt{\mu}}{2\nu\sqrt{3\nu + \mu}} + \frac{\sqrt{3\nu + \mu}}{2\nu\sqrt{\mu}} \\ \frac{\partial \mu_i}{\partial \beta}(\beta) &= \frac{\beta}{(1-u_i)^2} \left(\left(\frac{\beta}{1-u_i} \right)^2 + \frac{9\nu_i^2}{4} \right)^{-1/2} \end{aligned} \quad (14)$$

3.4 Degrees of freedom of the mixture of IG

The Bayesian Information Criteria (BIC, [35]) is used to chose the degrees of freedom (d.o.f.), namely the number of components of the mixture, which has been proven consistent for mixture models [7, 12, 33]. Therefore the chosen degree of freedom is equal to

$$K_i = \operatorname{argmax}_k 2\ell_n(\boldsymbol{\pi}_i, \boldsymbol{\beta}_i) - (2k - 1) \log n$$

where ℓ_n is the observed-data log-likelihood of an n -sample of response times. Thanks to the reparametrization of the previous section, and this degree of freedom, the number of parameters to estimate is reduced from $3K_i - 1$ to $2K_i - 1$.

3.5 Goodness-of-fit

We use the link of IG distributions of the jobs of a given task with the χ_1^2 distribution to check the quality of the MLE. Indeed, if X is an IG variable of mean ξ and shape δ , then $\delta(X - \xi)^2/\xi^2 X$ is distributed as a Chi-squared distribution of one degree of freedom [40]. Provided that the response time R_i is within the k -th component in the IG estimation, thus IG distributed, the foregoing normalization translates into the fact that normalized response time is Chi-squared distributed as follows

$$\frac{\left(R_i - \frac{\beta_{i,k}}{1-u_i}\right)^2}{\nu_i R_i} \sim \chi^2(1). \quad (15)$$

Therefore, we use (15) to test the MLE $\hat{\beta}_{i,k}$ goodness-of-fit to the empirical data, and provide the estimated failure rates. Note that the larger quantiles values are the ones that real-time designers are interested in to determine whether a task is weakly feasible or not.

Proposition 3. *The failure rate of the IG estimation is equal to*

$$\Delta_i^{IG} = \sum_{k=1}^{K_i} \pi_{i,k} \left| \mathbf{1} \left(p_i > \frac{\beta_{i,k}}{1-u_i} \right) - \Phi \left(\frac{\left(p_i - \frac{\beta_{i,k}}{1-u_i} \right)^2}{2\nu_i p_i} \right) \right| \quad (16)$$

where Φ is the c.d.f. of the $\chi^2(1)$ distribution.

Proof. See Appendix C. □

This formulation of the failure rates provides an easy and graphical way to see if the MLE calculated provide IG failure rates close enough the empirical ones. See in Figure 2 a comparison between the empirical failure rates, the IG method in (11) and the Hoeffding bound. When $u_i^{\max} < i(2^{1/i} - 1)$ the failure rate is zero (which is not the case with Hoeffding bounds).

3.6 Towards independence testing

As we do not investigate this topic, we still discuss the use of the Chi-squared property (15) to elaborate an independence test adapted to real-time systems. We have used in the foregoing section the central limit property of response times, coupled with the Chi-squared property of IG distributions, to build a goodness-of-fit criteria. Nevertheless, one could see response times as a statistic on execution times, that actually embed their dependence structure. With or without the EM estimation, the central limit of response times allows to build a chi-squared independence test with the following procedure :

1. Choose a task $\gamma_i \in \Gamma$,
2. Fit $(R_{i,j})_j$ -the response times n -sample- to an IG distributions, (we provide one way of doing this in this paper, but many other methods could be valid)
3. Extract the IG parameters $(\hat{\xi}_i, \hat{\delta}_i)$,
4. Check if $\sum_{j=1}^n \mathbf{P} \left(\frac{\hat{\delta}_i (R_{i,j} - \hat{\xi}_i)^2}{\hat{\xi}_i^2 R_{i,j}} > \Phi^{-1}(1 - \alpha) \right) \leq n\alpha$ for all $\alpha \in (0, 1)$.

The method provided in this paper strongly relies on the statistical independence of execution times. However, we have shown how to use it to also detect if execution time are indeed independent. We do not investigate in this paper the reliability of such method, but rather suggest that our method can also be useful in the case of dependent execution times.

4 Simulations

In this section, we apply the foregoing method with simulated data and hardware-in-the-loop (HITL) data.

4.1 Simulated data

Tab. 2: Parameters of the task set used for the simulations in Section 4.

Task priority	0	1	2	3	4	5	6	7	8	9
Mean execution time (ms)	15.481	5.556	5.708	3.38	5.198	4.057	4.998	3.786	2.167	7.453
Execution time std (ms)	17.1957	5.6996	5.9963	3.323	5.5314	4.0299	5.1184	3.9005	1.8259	8.3373
Periods (ms)	100	114	119	121	132	133	136	144	145	146
Mean utilization	0.1548	0.2035	0.2515	0.2794	0.3188	0.3493	0.3861	0.4124	0.4273	0.4784
Maximum utilization	0.28	0.3589	0.443	0.4926	0.5683	0.6285	0.702	0.7506	0.7713	0.874
Task priority	10	11	12	13	14	15	16	17	18	19
Mean execution time (ms)	16.812	1.833	2.167	2.7	5.448	8.46	2.167	4.665	2.4	5.604
Execution time std (ms)	19.1248	1.5271	1.8259	2.4495	5.4483	9.2277	1.8259	4.7411	2.2361	5.7741
Periods (ms)	159	165	165	165	166	173	181	182	183	191
Mean utilization	0.5841	0.5952	0.6083	0.6247	0.6575	0.7064	0.7184	0.744	0.7571	0.7865
Maximum utilization	1.0879	1.1061	1.1242	1.1485	1.2027	1.301	1.3175	1.3615	1.3834	1.4357
Task priority	20	21	22	23	24	25	26	27	28	
Mean execution time (ms)	2.333	3.334	5.927	4.535	4.225	6.246	4.779	2.167	1.834	
Execution time std (ms)	1.9147	3.0555	6.0701	4.4073	4.1931	6.758	4.8654	1.8259	1.4149	
Periods (ms)	193	200	201	214	215	268	296	298	315	
Mean utilization	0.7986	0.8152	0.8447	0.8659	0.8856	0.9089	0.925	0.9323	0.9381	
Maximum utilization	1.4513	1.4763	1.531	1.5637	1.6009	1.6494	1.6764	1.6865	1.696	

The simulated data is generated using SimSo [6], a Python framework used to generate arrivals of jobs and scheduling policies. A modified version of SimSo⁴ allows to generate random inter-arrival times (for the offset) and random execution times⁵. We study the quality of the estimation as a function of the mean utilization level. We show that when the mean utilization gets closer to 1, the estimation becomes better. We also check how much the IG bound is larger than the empirical failure rates,

$$\Delta_i^{(n)} = \frac{1}{n} \sum_{j=1}^n \mathbf{1}(R_{i,j} > p_i)$$

Consider a task set where the probability density functions of the execution times are known. We generate such task set with the UUnifast method [4, Section 3.6] and log-uniform periods according to the procedure described in [8, Section 6.1]. From SimSo we generate the response times of tasks with the RM scheduling policy from the execution time’s statistics given in Table 2. Two methods are used: one with a finite support where the maximal utilization u_i^{max} is finite, and another one with an infinite support with exponential distributions where the maximal utilization is not defined. This schedule is instantiated 1 000 times, thus in Figure 5, the distance between the MLE and simulations are based on 1 000 estimators. Also note in Figure 5 that the variability of the estimates decreases with respect to the mean utilization. Because of the static-priority structure of RM, we can see in Figure 5 that the error of the estimation decreases when the mean utilization goes to 1. The first task is never preempted, so its response time is always equal to its execution time. Therefore the estimation of its response time cannot be good in general.

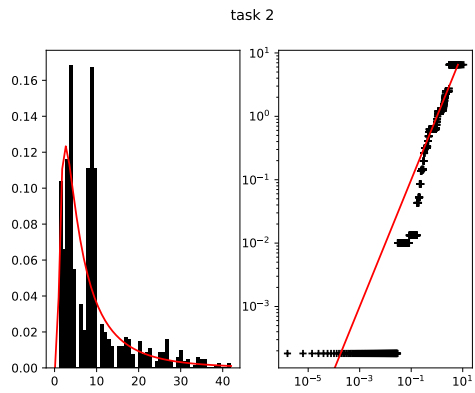
In a second step, a task set with exponentially distributed execution times is simulated for comparison (D/M/1/FP queue), as it is a special case widely studied in queueing theory [30]. This is a baseline to determine the convergence of the response times estimation as a function of the priority levels. This baseline confirms that the convergence depends on the type of distributions used for execution times, but that there is a phase transition at $u_i^{max} > 1$, independent from the type of distribution used for execution times. The parameters of the task set are given in Table 2. In Figure 2, we have the mean utilizations $(u_i)_i$ on the x -axis and the different failure rates on the y -axis.

We can see that when $u_i^{max} < i(2^{1/i} - 1)$, it is useless to compare the methods because they are already proven feasible in (5). Moreover, both start increasing when $u_i^{max} > 1$. Figure 5 confirms that in the region of interest, *i.e.* $u_i^{max} > 1$, the proposed estimation quadratic error between empirical and estimated distributions is close to 0 when $u_i^{max} > 1$, and goes to 0 when $u_i \rightarrow 1$, for any randomly generated task set: in this case the task set generated is shown in Table 2.

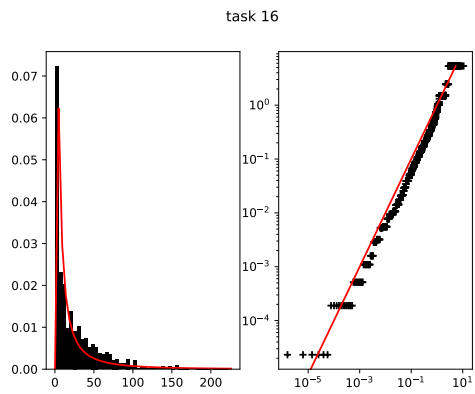
We see in Figure 4 the QQ-plots comparing the empirical quantiles and the quantiles of the χ_1^2 distributions introduced in Section 3.5. This figure shows two

⁴ <https://github.com/kevinzagalo/simso>

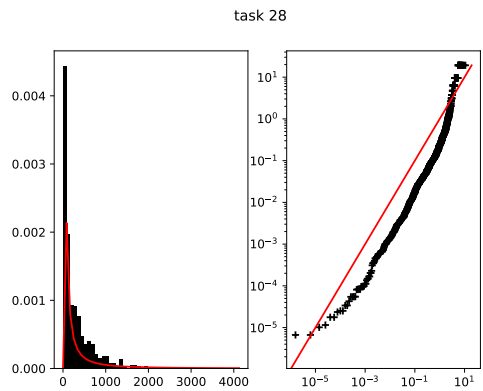
⁵ https://github.com/kevinzagalo/simso/blob/main/generator/task_generator.py



(a) Task 2



(b) Task 16



(c) Task 28

Fig. 4: The response time MLEs and the histogram of simulations from SimSo (left), and the associated QQ-plots (right) of empirical (x-axis) and $\chi^2(1)$ quantiles (y-axis) proposed in Section 3.5.

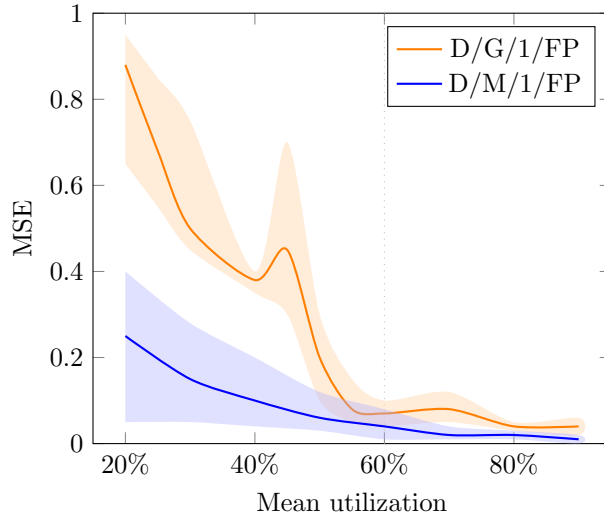


Fig. 5: Mean Squared Error (MSE) between the empirical distribution of the simulations and the MLE distribution, of 1000 instances of the schedule, for the task set shown in Table 2. This figure shows how the empirical response time data converges to the inverse Gaussian model when the mean utilization goes to 1, when assuming both the D/G/1/FP and D/M/1/FP models. The dotted line shows when the maximum utilization goes above 1.

things: as expected for the low priority tasks are not well estimated but are tight for higher tasks. Furthermore, the QQ-plots show that the proposed method is accurate and suited for response times distributions parametric estimation.

4.2 HITL Data

In this section we use the IG method on HITL data. Note that in this case, execution times are not necessarily independent. However, we test our method applied to real-data performs. We use a real case of 9 programs of an autopilot of a drone, PX4-RT [39], a modified version of PX4 [29] with a real-time behavior, and a clock-measuring that can preempt the operating system itself. PX4-RT is run on an ARM Cortex M4 CPU clocked at 180 MHz with 256 KB of RAM using a simulated environment from Gazebo [18]. PX4-RT allows to measure execution times and response times during the flight of a drone. It runs on top of NUTTX, a real-time operating system (RTOS). It provides an infrastructure for internal communications between all programs and off-board applications. Each task is a NUTTX task launched at the beginning of the PX4 program. The tasks read data from sensors (*snsr*), estimate positions and attitudes using a Kalman filter (*ekf2*), control the position (*pctl*) and the attitude (*actl*) of the drone, the flight manager (*fmgr*), the hover thrust estimator (*hte*), command

the state of the drone (*cmdr*), and the rate controller (*rcctl*), which is the innermost loop to control the body rates. These tasks are in constant interference with the operating system NUTTX, which makes them statistically dependent. Because the operating system has the highest priority, the nine tasks studied are constantly preempted by NUTTX. Unfortunately, it is not possible to get information about the operating system programs that interfere. Unlike the simulation in Section 4, PX4-RT runs concurrently with other tasks which do not have timing requirements, making it a complex system with many unknown variables. We test in this section whether and when the proposed parametric estimation is suitable for such complex system.

In this case, the distribution functions of execution times cannot be provided. Therefore, we use the empirical distributions whose statistics are shown in Table 3. The empirical mean utilizations \hat{u}_i are computed with the empirical means of execution times, and the empirical maximal utilizations \hat{u}_i^{max} with the empirical maximum of execution times. See Table 3 for a full description of the parameters. As shown in the previous section, the response times of the highest priority task *snr* are not estimated.

The QQplots in Figures 6a-6h show that the estimation is good for the large quantiles, which is what is important to determine the reliability. We can identify in Figure 6h Figure 6g and 6e that for the *cmdr*, *navr* and *fmgr* tasks the estimation is not good enough, which means that those programs are mutually dependent (operating system etc.), and that a feasibility test on this task would not be suitable with the method built in this paper. Nevertheless, for the other tasks the approximation is good and can therefore be used for a feasibility analysis.

5 Conclusion

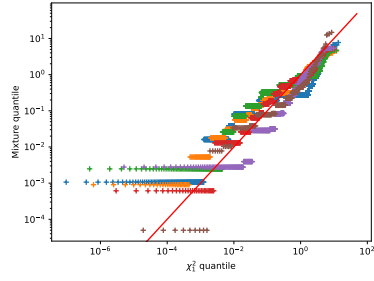
In this work, we both provide a theoretical and approximated bound on the failure rates of stationary rate-monotonic real-time systems. More than bounds, we provide a method that one could potentially improve scheduling algorithms, by estimating parameters with inference. We built this estimation through an EM algorithm, but this method is not unique, and hopefully some more techniques will improve the proposed method. Indeed, a current trend in real-time systems is the application of statistical learning methods in order to find optimal or improved policies [17, 20, 32, 37, 43]. In scheduling theory, the inference of *scheduling knowledge* [38] is a natural step into the application of the parametric method provided in this paper. The parametric estimation of new parameters, such as new virtual deadlines, help to improve the scheduling decisions. Multiple core real-time systems are a commonplace for these methods [34]. Shared resources are inherently a source randomness, and we think that multicore scheduling algorithm would benefit from incorporating the kind of method we build in this paper.

Tab. 3: Empirical parameters, periods and deadlines used in the autopilot PX4-RT described in Section 4.2.

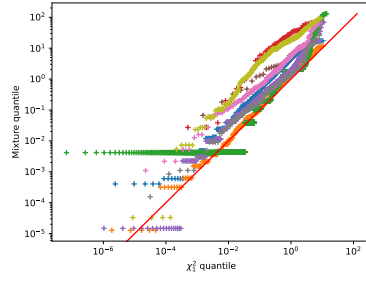
Task	snsr	retl	ekf2	actl	pctl	fmgr	hte	navr	cmdr
Priority i	1	2	3	4	5	6	7	8	9
Number of components	-	6	9	2	1	2	2	2	1
Empirical mean (μ_s)	152.5	44.2	610.9	38.7	52.5	151.0	30.61	159.8	114.4
Empirical std (μ_s)	40.5	16.4	982.8	9.5	32.6	114.4	10.9	133.9	61.6
Period (ms)	3.0	4.0	4.1	5.0	5.2	6.0	7.0	50.0	100.0
Deadline (ms)	3.0	4.0	4.1	5.0	5.2	6.0	7.0	50.0	100.0
Empirical mean utilization \hat{u}_i	0.05	0.06	0.21	0.22	0.23	0.25	0.26	0.26	0.26
Empirical maximum utilization \hat{u}_i^{max}	0.10	0.13	1.08	1.10	1.14	1.21	1.23	1.25	1.26
Empirical deadline miss probability	0.0	0.0	0.001	0.0	0.0	0.0	0.0	0.0378	0.0
IG deadline miss probability	-	0.0	0.0006	0.0043	0.028	0.0022	0.0009	0.5487	0.0
Hoeffding bound	-	10^{-168}	0.2512	0.1919	0.1881	0.1673	0.1274	10^{-7}	10^{-13}

References

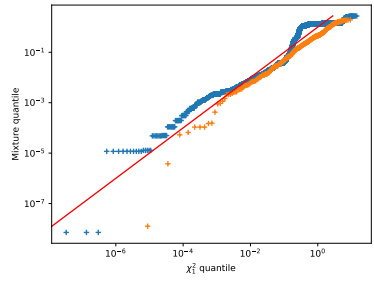
- [1] AC Aitken. Iii.—a series formula for the roots of algebraic and transcendental equations. *Proceedings of the Royal Society of Edinburgh*, 45(1):14–22, 1926.
- [2] Neil C Audsley, Alan Burns, Mike F Richardson, and Andy J Wellings. Hard real-time scheduling: The deadline-monotonic approach. *IFAC Proceedings Volumes*, 24(2):127–132, 1991.
- [3] Francois Baccelli and Pierre Brémaud. *Elements of queueing theory: Palm Martingale calculus and stochastic recurrences*, volume 26. Springer Science & Business Media, , 2013.
- [4] Enrico Bini and Giorgio C Buttazzo. Measuring the performance of schedulability tests. *Real-Time Systems*, 30(1):129–154, 2005.
- [5] Kuan-Hsun Chen, Georg Von Der Brüggem, and Jian-Jia Chen. Analysis of deadline miss rates for uniprocessor fixed-priority scheduling. In *2018 IEEE 24th International Conference on Embedded and Real-Time Computing Systems and Applications (RTCSA)*, pages 168–178. IEEE, 2018.
- [6] Maxime Chéramy, Pierre-Emmanuel Hladik, and Anne-Marie Déplanche. Simso: A simulation tool to evaluate real-time multiprocessor scheduling algorithms. In *Proc. of the 5th International Workshop on Analysis Tools and Methodologies for Embedded and Real-time Systems*, WATERS, 2014.
- [7] Abhijit Dasgupta and Adrian E Raftery. Detecting features in spatial point processes with clutter via model-based clustering. *Journal of the American statistical Association*, 93(441):294–302, 1998.
- [8] Robert I Davis and Alan Burns. Priority assignment for global fixed priority pre-emptive scheduling in multiprocessor real-time systems. In *2009 30th IEEE Real-Time Systems Symposium*, pages 398–409. IEEE, 2009.
- [9] José Luis Díaz, Daniel F García, Kanghee Kim, Chang-Gun Lee, L Lo Bello, José María López, Sang Lyul Min, and Orazio Mirabella. Stochastic analysis of periodic real-time systems. In *23rd IEEE Real-Time Systems Symposium, 2002. RTSS 2002.*, pages 289–300. IEEE, 2002.
- [10] Bogdan Doytchinov, John Lehoczky, and Steven Shreve. Real-time queues in heavy traffic with earliest-deadline-first queue discipline. *Annals of Applied Probability*, pages 332–378, 2001.
- [11] J Leroy Folks and Raj S Chhikara. The inverse gaussian distribution and its statistical application—a review. *Journal of the Royal Statistical Society: Series B (Methodological)*, 40(3):263–275, 1978.
- [12] Chris Fraley and Adrian E Raftery. Model-based clustering, discriminant analysis, and density estimation. *Journal of the American statistical Association*, 97(458):611–631, 2002.



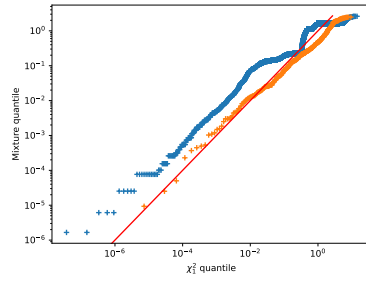
(a) *rctl*



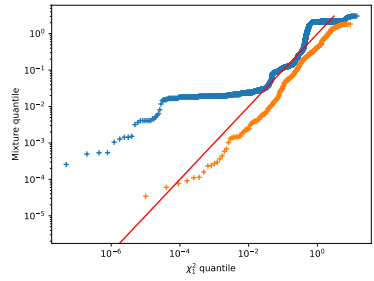
(b) *ekf2*



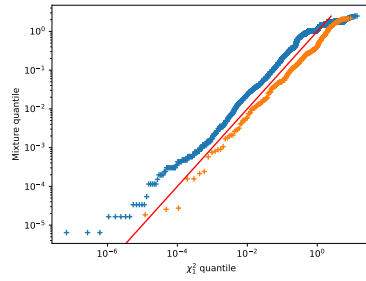
(c) *actl*



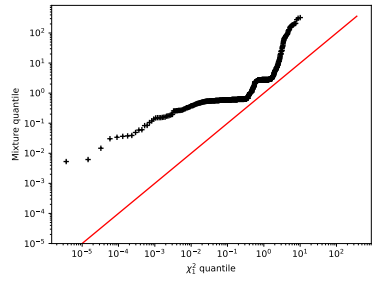
(d) *pctl*



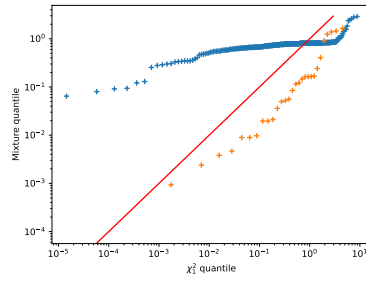
(e) *fmgr*



(f) *hte*



(g) *navr*



(h) *cmdr*

Fig. 6: QQplot with the χ^2_1 quantiles from (15) where each color represents a component of the mixture. The closer to the red line the better the estimation.

- [13] Anna Friebe, Tommaso Cucinotta, Filip Marković, Alessandro Vittorio Papadopoulos, and Thomas Nolte. Nip it in the bud: Job acceptance multi-server. In *2025 IEEE 31st Real-Time and Embedded Technology and Applications Symposium (RTAS)*, pages 26–39. IEEE, 2025.
- [14] Anna Friebe, Filip Marković, Alessandro V Papadopoulos, and Thomas Nolte. Efficiently bounding deadline miss probabilities of markov chain real-time tasks. *Real-Time Systems*, 60(3):443–490, 2024.
- [15] Anna Friebe, Filip Marković, Alessandro Vittorio Papadopoulos, and Thomas Nolte. Continuous-emission markov models for real-time applications: Bounding deadline miss probabilities. In *2023 IEEE 29th Real-Time and Embedded Technology and Applications Symposium (RTAS)*, pages 14–26. IEEE, 2023.
- [16] Zhiyun Jiang, Tianming Zhao, Chunqiu Xia, Wei Li, and Albert Y. Zomaya. The cost of accurate predictions in learning-augmented scheduling. In *2025 IEEE 31st International Conference on Embedded and Real-Time Computing Systems and Applications (RTCSA)*, pages 221–232, 2025.
- [17] Nagesh Kadaba, Kendall E Nygard, and Paul L Juell. Integration of adaptive machine learning and knowledge-based systems for routing and scheduling applications. *Expert Systems with Applications*, 2(1):15–27, 1991.
- [18] Nathan Koenig and Andrew Howard. Design and use paradigms for gazebo, an open-source multi-robot simulator. In *2004 IEEE/RSJ International Conference on Intelligent Robots and Systems (IROS)(IEEE Cat. No. 04CH37566)*, volume 3, pages 2149–2154. IEEE, 2004.
- [19] Phillip A Laplante et al. *Real-time systems design and analysis*. Wiley New York, , 2004.
- [20] C-Y Lee, Selwyn Piramuthu, and Y-K Tsai. Job shop scheduling with a genetic algorithm and machine learning. *International Journal of production research*, 35(4):1171–1191, 1997.
- [21] Edward A Lee. Cyber physical systems: Design challenges. In *2008 11th IEEE international symposium on object and component-oriented real-time distributed computing (ISORC)*, pages 363–369. IEEE, 2008.
- [22] John P Lehoczky. Real-time queueing theory. In *17th IEEE Real-Time Systems Symposium*, pages 186–195. IEEE, 1996.
- [23] John P Lehoczky. Using real-time queueing theory to control lateness in real-time systems. *ACM SIGMETRICS Performance Evaluation Review*, 25(1):158–168, 1997.

- [24] Chung Laung Liu and James W Layland. Scheduling algorithms for multiprogramming in a hard-real-time environment. *Journal of the ACM (JACM)*, 20(1):46–61, 1973.
- [25] Filip Marković, Thomas Nolte, and Alessandro Vittorio Papadopoulos. Analytical approximations in probabilistic analysis of real-time systems. In *2022 IEEE Real-Time Systems Symposium (RTSS)*, pages 158–171. IEEE, 2022.
- [26] Filip Marković, Alessandro Vittorio Papadopoulos, and Thomas Nolte. On the convolution efficiency for probabilistic analysis of real-time systems. In *33rd Euromicro Conference on Real-Time Systems (ECRTS)*. Schloss Dagstuhl–Leibniz-Zentrum für Informatik, 2021.
- [27] Filip Markovic, Pierre Roux, Sergey Bozhko, Alessandro V Papadopoulos, and Björn B Brandenburg. Cta: A correlation-tolerant analysis of the deadline-failure probability of dependent tasks. In *Proceedings of the 44th IEEE Real-Time Systems Symposium (RTSS)*, 2023.
- [28] Geoffrey J McLachlan, Sharon X Lee, and Suren I Rathnayake. Finite mixture models. *Annual review of statistics and its application*, 6:355–378, 2019.
- [29] Lorenz Meier, Dominik Honegger, and Marc Pollefeys. Px4: A node-based multithreaded open source robotics framework for deeply embedded platforms. In *2015 IEEE International Conference on Robotics and Automation (ICRA)*, pages 6235–6240, 2015.
- [30] Charles D Pack. The output of a d/m/1 queue. *SIAM Journal on Applied Mathematics*, 32(3):571–587, 1977.
- [31] Antonio Punzo. A new look at the inverse gaussian distribution with applications to insurance and economic data. *Journal of Applied Statistics*, 46(7):1260–1287, 2019.
- [32] Manish Purohit, Zoya Svitkina, and Ravi Kumar. Improving online algorithms via ml predictions. *Advances in Neural Information Processing Systems*, 31, 2018.
- [33] Adrian E Raftery. Bayesian model selection in social research. *Sociological methodology*, pages 111–163, 1995.
- [34] Shaima Rahim, Piyoosh Purushothaman Nair, and Rajesh Devaraj. A survey of machine learning-driven task scheduling approaches for multiprocessor systems. *Journal of Systems Architecture*, 171:103628, 2026.
- [35] Gideon Schwarz. Estimating the dimension of a model. *The annals of statistics*, pages 461–464, 1978.

- [36] Venkata Seshadri. *The inverse Gaussian distribution: statistical theory and applications*, volume 137. Springer Science & Business Media, , 2012.
- [37] Rana Shahout and Michael Mitzenmacher. Skippredict: When to invest in predictions for scheduling. In A. Globerson, L. Mackey, D. Belgrave, A. Fan, U. Paquet, J. Tomczak, and C. Zhang, editors, *Advances in Neural Information Processing Systems*, volume 37, pages 105663–105701, 2024.
- [38] M. J. SHAW, S. PARK, and N. RAMAN. Intelligent scheduling with machine learning capabilities: The induction of scheduling knowledge. *IIE Transactions*, 24(2):156–168, 1992.
- [39] Yves Sorel, Ismail Hawila, Liliana Cucu-Grosjean, Mehdi Mezouak, Hadrien Clarke, and Slim Ben-Amor. Kopernic dynamic benchmarks (kdbench)-open source measurement-based benchmarks. In *RTSS@ work 2024-organized as part of the IEEE Real-Time Systems Symposium (RTSS) 2024*, 2024.
- [40] Maurice CK Tweedie. Statistical properties of inverse gaussian distributions. i. *The Annals of Mathematical Statistics*, 28(2):362–377, 1957.
- [41] Georg von der Brüggen, Nico Piatkowski, Kuan-Hsun Chen, Jian-Jia Chen, and Katharina Morik. Efficiently approximating the probability of deadline misses in real-time systems. In *30th Euromicro Conference on Real-Time Systems (ECRTS 2018)*. Schloss Dagstuhl-Leibniz-Zentrum fuer Informatik, 2018.
- [42] Abraham Wald. On Cumulative Sums of Random Variables. *The Annals of Mathematical Statistics*, 15(3):283 – 296, 1944.
- [43] Alexander Wei and Fred Zhang. Optimal robustness-consistency trade-offs for learning-augmented online algorithms. *Advances in Neural Information Processing Systems*, 33:8042–8053, 2020.
- [44] Kevin Zagalo, Yasmina Abdeddaïm, Avner Bar-Hen, and Liliana Cucu-Grosjean. Response time stochastic analysis for fixed-priority stable real-time systems. *IEEE Transactions on Computers*, pages 1–12, 2022.

A Proof of Proposition 1

From Lemma 1 and 2 in [44], we get that, with $C_{i,j} = x$ and $\sum_{k=1}^{i-1} \beta_k(A_{i,j}) = y$, $R_{i,j}$ converges to an inverse Gaussian variable of mean $\frac{x+y}{1-u_i}$ and variance $\frac{(x+y)^2}{v_i^2}$ when u_i gets close to 1. We conclude with the fact that $\sum_{k=1}^i \beta_k(A_{i,j}) = C_{i,j} + \sum_{k=1}^{i-1} \beta_k(A_{i,j})$.

B Proof of Proposition 2

Let us consider a task γ_i where $i > 1$. Firstly let us remark that $R_{i,j}$ is upper-bounded with probability 1 as shown in (17).

$$R_{i,j} \leq \inf\{t > 0 : \sum_{k=1}^i \beta_k(A_{i,j}) + W_{k-1}(t + A_{i,j}) - W_{k-1}(A_{i,j}) \leq t\} \quad (17)$$

Thanks to the discarding policy, there cannot be more than one job per task activated at the same time. Thus, the tail function of $R_{i,j}$ is upper-bounded as shown in (18).

$$\mathbf{P}(R_{i,j} > t) \leq \mathbf{P}\left(\sum_{k=1}^{i-1} C_{k,N_k(A_{i,j})} + C_{i,j} + W_{i-1}(t + A_{i,j}) - W_{i-1}(A_{i,j}) > t\right) \quad (18)$$

From the stationarity of all demand processes $(W_i)_i$, we get that

$$\begin{aligned} & \mathbf{P}\left(\sum_{k=1}^{i-1} C_{k,N_k(A_{i,j})} + C_{i,j} + W_{i-1}(t + A_{i,j}) - W_{i-1}(A_{i,j}) > t\right) \\ &= \mathbf{P}\left(\sum_{k=1}^{i-1} C_{k,N_k(A_{i,j})} + C_{i,j} + W_{i-1}(t) - W_{i-1}(0) > t\right). \end{aligned}$$

Since $\mathbf{P}(N_i(0) = 0) = 1$ for all the tasks $(\gamma_i)_i$ we finally get the upper-bound

$$\mathbf{P}(R_{i,j} > t) \leq \mathbf{P}\left(\sum_{k=1}^{i-1} C_{k,N_k(A_{i,j})} + C_{i,j} + W_{i-1}(t) > t\right).$$

Since the execution times of a task are i.i.d., and independent from the execution time of other tasks,

$$\begin{aligned} & \mathbf{P}\left(\sum_{k=1}^{i-1} C_{k,N_k(A_{i,j})} + C_{i,j} + W_{i-1}(t) > t\right) \\ &= \mathbf{P}\left(\sum_{k=1}^i C_k + W_{i-1}(t) > t\right). \end{aligned}$$

The processes $(N_i)_i$ are mutually independent and also independent from $C_{i,1}$. Finally all the variables $C_{i,j}$ are in $[c_i^{min}, c_i^{max}]$ with probability 1. Thus according to Hoeffding's inequality we get the following upper-bound on the conditionnal probability in (19).

$$\mathbf{P}\left(\mathbf{P}(R_{i,j} > t \mid N_1(t), \dots, N_i(t)) \leq \exp\left(-2 \frac{(t - \mathbf{E}[\sum_{k=1}^i C_k + W_{i-1}(t)])^2}{\sum_{k=1}^i (c_k^{max} - c_k^{min})^2 N_i(t)}\right)\right) = 1 \quad (19)$$

Let $t \in (0, p_i)$. Since only one job of γ_i is released before p_i , we have $W_{i-1}(t) = \sum_{k=1}^{i-1} \sum_{j=1}^{N_k(t)} C_{k,j}$ and

$$\mathbf{E}[W_{i-1}(t)] = \sum_{k=1}^{i-1} \mathbf{E}[N_k(t)] \mathbf{E}[C_k] = \sum_{k=1}^{i-1} (\lambda_k t) \mathbf{E}[C_k] = u_{i-1} t \quad (20)$$

by Wald's lemma [42]. For any $t \geq 0$, $N_{i-1}(t)$ satisfies

$$(\lambda_{i-1} t - 1)^+ \leq N_{i-1}(t) \leq \lambda_{i-1} t + 1. \quad (21)$$

Hence, for $u_{i-1} < 1$, and from the RHS of (21), we get

$$u_{i-1} t + 2 \sum_{k=1}^i \mathbf{E}[C_k] \geq \mathbf{E}[W_{i-1}(t) + \sum_{k=1}^i C_k],$$

which implies that, $t > \mathbf{E}[W_{i-1}(t) + \sum_{k=1}^i C_k]$ if $t > \frac{2 \sum_{k=1}^i \mathbf{E}[C_k]}{1 - u_{i-1}}$. We are interested in the case $t = p_i$. Suppose $p_i > \frac{2 \sum_{k=1}^i \mathbf{E}[C_k]}{1 - u_{i-1}}$. With (21) and (20) we get

$$\begin{aligned} & \frac{(p_i - \mathbf{E}[W_{i-1}(p_i) + \sum_{k=1}^i C_k])^2}{\sum_{k=1}^i (c_k^{max} - c_k^{min})^2 N_k(p_i)} \\ & \geq \frac{p_i^2 (1 - u_{i-1} + \lambda_i \sum_{k=1}^i \mathbf{E}[C_k])^2}{\sum_{k=1}^i (c_k^{max} - c_k^{min})^2 \lambda_k p_i + \sum_{k=1}^i (c_k^{max} - c_k^{min})^2} \\ & = \frac{p_i (1 - u_{i-1} + \lambda_i \sum_{k=1}^i \mathbf{E}[C_k])^2}{(v_i^{max})^2 + \lambda_i \sum_{k=1}^i (c_k^{max} - c_k^{min})^2}. \end{aligned}$$

Since we are using the RM policy, we have $\lambda_k \geq \lambda_i$ for $i \geq k$, hence we get

$$(v_i^{max})^2 + \lambda_i \sum_{k=1}^i (c_k^{max} - c_k^{min})^2 \leq 2(v_i^{max})^2.$$

Furthermore, $1 - u_{i-1} > 2\lambda_i \sum_{k=1}^i \mathbf{E}[C_k]$ which gives us the result with the fact that $x \rightarrow \exp(-x)$ is decreasing. We conclude by noticing that the RHS in (19) does not depend on j , hence it holds for all jobs of the task γ_i .

C Proof of Proposition 3

Since $g(r; \theta) = \frac{(r-\theta)^2}{r}$ is positive and, decreasing w.r.t. to r , for $r \leq \theta$ and increasing for $r > \theta$, we get the result using (15) with (11) and $\theta = \frac{\beta}{1-u_i}$ and $x = g(r; \theta)$.